Journal of King Saud University – Science 32 (2020) 3372–3379

Contents lists available at ScienceDirect

Journal of King Saud University – Science

journal homepage: www.sciencedirect.com

Original article

Green biosynthesis of silver nanoparticle using *Commiphora myrrh* extract and evaluation of their antimicrobial activity and colon cancer cells viability

Mona S. Alwhibi [a], Dina A. Soliman [a,*], Hala al khaldy [a], Aljohara Alonaizan [a], Najat Abdulhaq Marraiki [a], Mohamed El-Zaidy [a], Moodi S. AlSubeie [b]

[a] Department of Botany and Microbiology, King Saud University, P. O. Box: 22452, Riyadh 11495, Saudi Arabia
[b] Mohammad Ibn Saud Islamic University College of Science, Riyadh Department of Biology, Saudi Arabia

ARTICLE INFO

Article history:
Received 6 April 2020
Revised 10 September 2020
Accepted 20 September 2020
Available online 6 October 2020

Keywords:
Antimicrobial
AgNPs
Colon cancer
Commiphora myrrha
Green biosynthesis

ABSTRACT

There is increasing attention directed to mineral nanoparticle for intensive applications in various fields of science, such as medicine, chemistry, agriculture, and biotechnology. There is also a growing attentiveness to the use of eco-friendly methods to synthesize nanoparticle without making or using environmentally dangerous substances to human health. This article describes the biological methods for green synthesis using *Commiphora myrrha* silver nanoparticle (AgNP) extract. C. myrrha-synthesized AgNPs, which were completed by exposing myrrh aqueous extract to silver nitrate, were characterized by transmission electron microscopy, Fourier transform infrared spectroscopy, Zetasizer, and ultraviolet–visible spectral analyses. AgNPs were characterized by varying the color of the solution from light yellow to brown and then depicting the surface plasmon-resonance peaks at 445 nm. This study has promising results in the treatment of colon cancer, as it has impressive outcomes using different concentrations of AgNPs in 100 µl medium (30%) compared to control (100%). The results also showed increasing inhibition zones of antibacterial activity with AgNPs in *Enterococcus faecalis* (59 mm) and *Bacillus cereus* (51 mm) compared to myrrh aqueous extract. Fungi that were screened for growth inhibition zones were Fusarium oxysporum (20 mm), *Alternaria alternata* (14 mm), and *Trichoderma* (10 mm).

1. Introduction

Commiphora myrrha belongs to the genus *Commiphora* and family Burseraceae (Su et al., 2011). Myrrh consists of alcohol-soluble resins (25–40%), volatile oils (3–8%), and water-soluble gum (30–60%; (Tucker, 1986; Hanuš et al., 2005; Mekonnen, 2014). The latter consists of proteins and polysaccharides, whereas volatile oils comprise a mixture of terpenes, sterols, and steroids (Hanuš et al., 2005). Plant substances are biochemical mixtures formed in plants called minor derivatives of metabolic movements, which consist of alkaloids, turbines, phenols, and others that have unlimited importance to human production, such as medicine, leather dyeing, soap, haul-out essential oils, food, and cosmetic industries, and protein, carbohydrate, and fat metabolism (Judd et al., 2002). Substances are excreted to protect the plant from external invasion from microbes and insects and act as the plant's immune system, which look like brown spots that appear as sickness or insect infestation. *C. myrrha* (Nees) Engl. (Burseraceae) is native to Madagascar, Arabian islands, and India. To collect the resin, inhabitants form cracks in the bark to produce wounds from which a milky white substantial dries out, solidifies, and turns rosy brown after exposure to air (Ben-Yehoshua et al., 2012).

At present, the trend of natural alternative medicine has improved worldwide, and *C. myrrha* has been reevaluated and is used as a laxative and for curative cuts with ulcers. Traditionally, *C. myrrha* is used as a bandage for skin ulcers and sores and in the management of tonsillitis and gingivitis; it is also used to treat cough and as a quick-acting medicine for cough with mucus and bronchitis (El Ashry et al., 2003).

* Corresponding author.
E-mail address: dsoliman@ksu.edu.sa (D.A. Soliman).
Peer review under responsibility of King Saud University.

Production and hosting by Elsevier

https://doi.org/10.1016/j.jksus.2020.09.024
1018-3647/

Myrrh aqueous extract is used as a maintenance drug, which is accepted by the Food and Drug Administration, and also used in food as a flavor component (Ford et al., 1992).

Metal nanoparticle synthesis has received increasing attention due to its wide range of use in the fields of medicine, energy, and electronics (Saxena et al., 2012; Biswal and Misra, 2020). Studies have been made to explore their utilization and properties for practical use, such as antibacterial drugs and anticancer therapy (Le Ouay and Stellacci, 2015; Biswal and Misra, 2020). One of the most important types of metal nanoparticle is liquid; it is made from noble metals such as silver, platinum, and gold (Kaviya et al., 2011).

Among the metal nanoparticle, silver nanoparticle (AgNPs) are well known for their use in photonics (Gould et al., 2000; Hösel and Krebs, 2012; Inácio et al., 2013), microelectronics (De Heer, 1993; Reddy et al., 2007), photocatalysis (Bawendi et al., 1990; Bar et al., 2009), and lithography (Xia et al., 1999; Shipway et al., 2000).

The use of AgNPs in medicine is recognized for their effective antimicrobial activity against various kinds of pathogenic microbes (Klaine et al., 2008).

AgNPs have a wide range of uses, and silver has been widely used as a colloidal material. Due to advances in technology, the synthesis, development, and characterization of novel products have become easier. The fields for their applications range from drug delivery, biosensing, and nanomedicine to catalysis, nanodevice fabrication, and imaging.

In this paper, we report the production of AgNPs using various biological and physiochemical methods, the promising applications of AgNPs in biomedicine from nanomedicine to optoelectronics, and their antibacterial, antifungal, and anticancer activities.

2. Material and method

2.1. Preparation of myrrh aqueous extract

Myrrh was obtained from a local market in Riyadh, Saudi Arabia. Myrrh was then washed using distilled water, air-dried, and ground to powder. About 10 g powder was added to a 500 ml conical flask with 200 ml triple-deionized water, mixed well using a magnetic stirrer, and then incubated to a 65 °C water bath for 5 h. The resulting component was centrifuged at 5000 rpm for 15 min and then filtered using Whatman filter paper no. 1. The filtrate was kept at 4 °C for further use.

2.2. Synthesis of AgNPs

The silver nitrate ($AgNO_3$) aqueous solution (10 mM) was prepared using $AgNO_3$ powder and triple-deionized water in a fixed ratio. The reaction was prepared by taking 10 ml of the above-prepared filtrates obtained from myrrh and 90 ml $AgNO_3$ solution and then incubated at room temperature for 3 h. A small amount of the reaction mixture was centrifuged at 20,000 rpm for 15 min (Fig. 1).

2.3. Characterization of AgNPs

The plasmon-resonance property of synthesized AgNPs was studied using an ultraviolet–visible (UV–vis)/near-infrared (NIR) spectrophotometer (Perkin 750, USA). The AgNP sample was first sonicated for uniform scattering, and the aqueous solution was analyzed at room temperature for the plasmon-resonance property. JEOL-JEM-1011 transmission electron microscopy (TEM) was used to characterize the size and shape of AgNPs. The impurity content was characterized by Fourier transform infrared (FTIR) spectroscopy using a Nicolet 6700 FT-IR instrument (Thermo Scientific; Biswal and Misra, 2020).

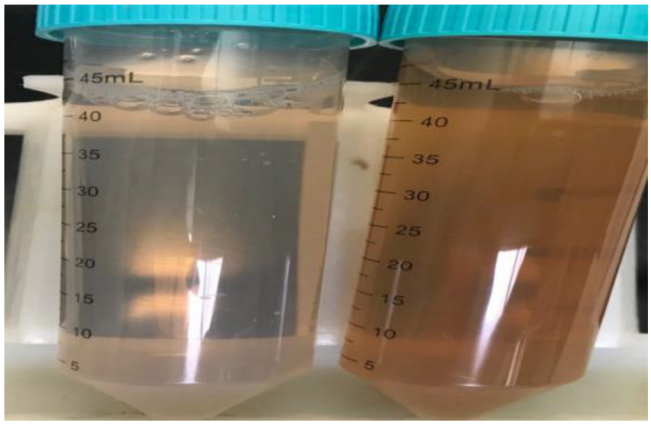

Fig. 1. Showing a color of the solution of Ag NPs with myrrh extract as green-reducing, (A) after 5 min and (B) after 3 h.

2.4. Biological activities of AgNPs

2.4.1. Anticancer activity

The cancer cell clone line was provided by King Saud University Central Lab, Girl's Campus (Riyadh, Saudi Arabia). AQueous One Solution Cell Proliferation Assay (Promega) was added at 37 °C to a final concentration of 5 mg/ml. The colon cancer cell line (SW480) cells were seeded in a 96-well plate in 2 × 105 cells/well density in 100 µl enhanced medium. The total cell number used in the different experiments was determined using a cell counter. Cells were treated with individual concentrations of AgNPs (3.125, 6.25, 12.5, 50, and 100 µl). The treated cells were allowed to grow for 48 h. After incubation and concentration point, 20 µl Cell Titer 96® AQueous One Solution Cell Proliferation Assay was added at 37 °C to a final concentration of 5 mg/ml. The 96-well plate was kept in the dark for 2 h. The optical density of each treatment was measured at 490 nm using a 96-well plate reader (Molecular Devices (SpectraMax). Data are represented as the mean ± standard deviation (n = 3).

2.4.2. Antibacterial activity

Nutrient agar medium (14 g powder dissolved in 500 ml distilled water) was then autoclaved. The agar was poured at 20 ml in each Petri dish and allowed to solidify for 15 min, and the plates were incubated overnight with human pathogens. Gram-negative strain, such as *Escherichia coli* (negative) ATCC35218, and Gram-positive strains, such as *Staphylococcus aureus* ATCC 43300, *Enterococcus faecalis* ATCC 29212, and *Bacillus cereus* ATCC 11778 (clinical isolate), were obtained from King Khalid University Hospital (Riyadh, Saudi Arabia). The medium was softly beaten using a sterile cork-borer to make two wells in each plate, with two equal dimensions from the center of the dish. Then, AgNPs synthesized by myrrh aqueous extract and pure myrrh extract were added separately in each hole until the well was flooded, and the medium was incubated at 37 °C for 24 h. The diameter of the zone of inhibition was measured after incubation and expressed in millimeters.

2.4.3. Antifungal activity

The extracts were assayed for antifungal activity against *Alternaria alternata, Fusarium oxysporum*, and *Trichoderma*. The fungi were grown on a potato dextrose agar plate at 28 °C. Then, 500 ml medium was prepared using 19 g in 500 ml distilled water

and autoclaved. AgNPs synthesized by myrrh aqueous extract and pure myrrh extract were added separately in each dish before transfer into sterile Petri dishes and mixed gently for testing. A 6-mm-diameter fungal disc with 7-day-old cultures of the incubated for 7 days at 28 °C. The medium without nanoparticle served as a control. The antifungal activity was estimated by measuring the diameter and expressed as the percentage inhibition of mycelial growth. Percentage inhibition was taken on the seventh day and on the day when the mycelial growth in the control plate reached the edge of the Petri dish.

3. Results and discussion

3.1. UV–vis spectral analysis

The plasmon-resonance property of synthesized AgNPs was studied using UV–vis/NIR spectrophotometry. The synthesized nanoparticle sample was first sonicated for uniform dispersion, and the aqueous solution was analyzed at room temperature for the plasmon-resonance property. Visual observation and UV–vis spectroscopy of AgNPs Fig. 2 (A) were effectively performed via a bioreduction method using *Commiphora* at a maximum of 445 nm Fig. 2 (B) spectral /of the extract are in the range of 282–285 nm while Ag NPs formed by both method have a peak wavelength of 445 nm. plasmon surface vibrations in AgNPs (Bawendi et al., 1990). UV–vis spectroscopy allowed the detection of the color change (Bar et al., 2009) throughout the reduction of Ag ions to AgNP with *C. myrrha* plant extract. Plasmon surface vibrations in AgNPs (Bawendi et al., 1990). UV–vis spectroscopy allowed the detection of the color change (Bar et al., 2009) throughout the reduction of Ag ions to AgNPs with *C. myrrha* plant extract. These changes are due to the rapid change of the surface plasmon resonance of AgNPs. This change is denoted by the broadening of the peak, which indicates the formation of polydispersed large A nanoparticle due to slow reduction rates.

3.2. FTIR analysis

FTIR shows the biomolecules supplemented with AgNPs and the corresponding absorption peaks for O–H groups of phenols and C–H aromatic stretch at ~3290 and 1635 cm^{-1}, respectively (Fig. 3). Together with TE images (Bar et al., 2009), synthesized nanoparticle by plant extracts are encircled by a tiny layer of organic substances that appeared on the plants 6 weeks after their synthesis; perhaps due to the covering material on the particle (Ahmad et al., 2015; Ramteke et al., 2012). FTIR shows AgNPs synthesized by myrrh aqueous extract. AgNPs (Fig. 3A) showed absorption at 3264.32, 2202.2, 2246.38, 2032.89, 2017.91, 2005.85, 2166.98, 2144.5, 1961.83, 1636.98, 453.64, and 430.54 cm. The absorption peak at 3264.32 cm^{-1} corresponds to the (OH) group, the peaks at 2166.98 and 2144.50 cm^{-1} correspond to (-C≡C-) alkyne, the peak at 1636.98 cm^{-1} corresponds to (N–H), and the peak at 1961.83 cm^{-1} corresponds to (=C–H). In (Fig. 3B), the peak at 2185.12 cm^{-1} disappeared in the AgNP absorption bands; therefore, this peak (2185.12 cm^{-1}), which corresponds to (C≡C) alkyne, might have helped *C. myrrha* to produce nanoparticle (Feng et al., 2000). Figure (3C) compares between the curves of Figs. 3A and 3B.

3.3. Zeta sizer analysis

The size of the nanoparticle was measured by Zetasizer (Fig. 4) at the Central Laboratory of King Saud University. The average size of AgNPs was 22 nm, which was used to determine the mean Z-average (diameter in nanometers) of AgNPs. As shown in Fig. 4, the mean average size of the resulting nanoparticle was 22.57 nm. The size distribution profile of AgNPs showed three significant peaks at 37.21, 3.19, and 2574 nm. The intensities were 88.5%, 9.3%, and 2.2%. The polydispersity index of the AgNP suspension was 0.502, indicating that the synthesized particle varied in size and showed little agglomeration.

3.4. TEM

Fig. 5 shows the TEM images of the synthesized AgNPs. The images clearly show that comparatively circular nanoparticle are designed with an average diameter between 0.5 and 25 nm, with some deviations. TEM images presented that the shape of the produced AgNPs is spherical with little agglomeration and various sizes. As shown in Fig. 5, the silver nanoparticle's diameter was 0.151 nm and 0.226 nm. This agglomeration was due to the aggre-

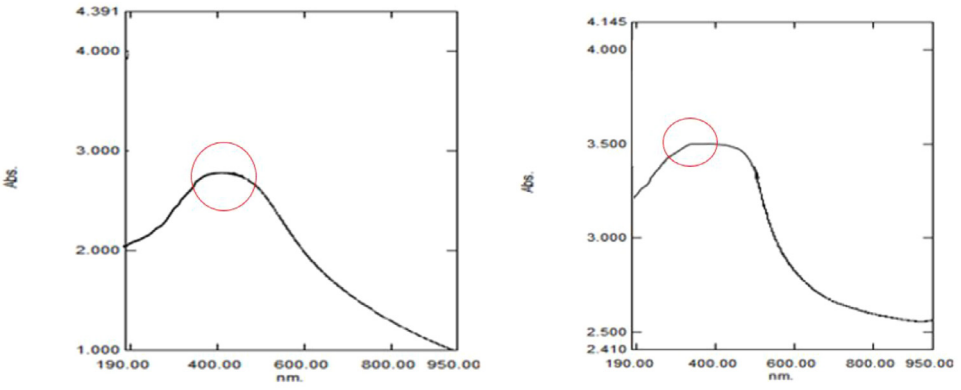

Fig. 2. UV–Vis spectra of Ag NPs produ ced by myrrh extract shows (A) spectral analysis of the absorption of silver nanoparticles at top 445 nm and (B) by myrrh extract only the absorption at 285 nm.

gation and adsorption of the compounds found in the extract onto the AgNP surface (Biswal and Misra, 2020).

3.5. Biomedical applications

3.5.1. Anticancer activity

Fig. 6 shows the highest concentration of nanoparticle for the treatment of colon cancer cells, which helped reduce cell viability. When the treatment used a concentration of 100 µl, the viability of the cancer cells was 30%. In comparison, the viability was 50% when the treatment used a concentration of 12.5 µl compared to control; the nanoparticle extract had 100% viable cells during 48 h incubation. Cytotoxicity assessments were performed using 3-(4,5-dimethyl thiazol-2-yl)-2,5-diphenyltetrazolium bromide (MTT) (Babich and Borenfreund, 1987). The MTT colorimetric assay is based on the mitochondrial dehydrogenase enzyme of the viable cells. The nanoparticle synthesized from the myrrh aqueous extract had cytotoxic responses, suggesting that synthesized AgNPs could contribute in the search of an alternative chemotherapeutic agent. Using the MTT test, the results depend on the enzyme hydrogenic mitochondria for living cells, which is destroyed by the nanocomposite.

3.5.2. Antibacterial activity

The antibacterial activity against *E. coli* (30 mm) and *S. aureus* (45 mm) has minimum zones of inhibitions due to the maximum capacity of the bacterial isolates. A widespread range of inhibition was observed against *E. faecalis* (59 mm) and *B. cereus* (51 mm; Fig. 7). Silver has been long known for its wide-ranging antimicrobial activity against Gram-positive and Gram-negative bacteria in addition to resistant strains (Bar et al., 2009; Xia et al., 1999). Silver can be applied in a wide range of applications to decrease

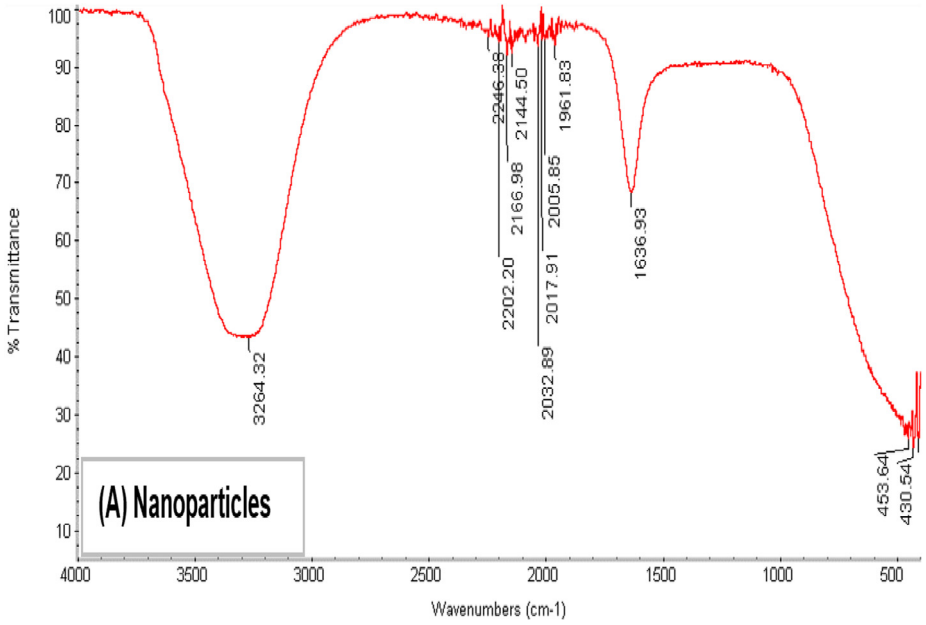

Fig. 3A. Showing FTIR spectra Ag NPs synthesized using extract of myrrh.

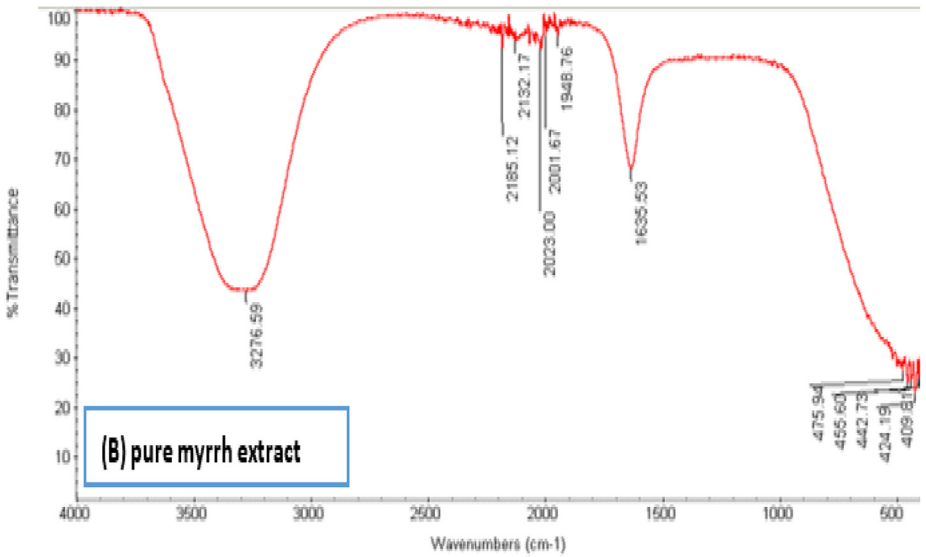

Fig. 3B. Showing FTIR spectra pure extract of myrrh.

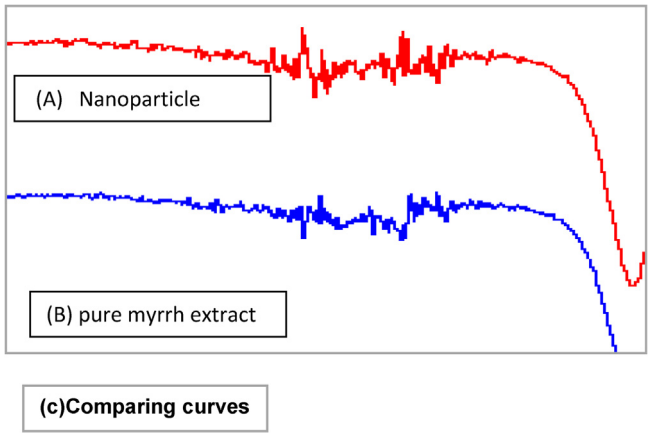

Fig. 3C. Showing FTIR spectra a) Ag NPs synthesized using extract of myrrh, b) pure extract of myrrh, c) the comparing between the a) and b) curves.

infections and eliminate bacteria on food packaging, medicinal procedures, material cloths, and water treatment (Jensen et al., 2000; Klaine et al., 2008; Lu et al., 2003; Lukman et al., 2011; Saifuddin et al., 2009; Shipway et al., 2000; Tsuji et al., 2003). AgNPs exhibited antimicrobial effects against bacterial cells via (a) membrane damage through association/interaction of AgNPs with DNA and biomolecules, leading to the inhibition of cell multiplication, and (b) reactive oxygen species formation through interaction with enzymes and/or biomolecules, leading to cell damage/destruction (Noginov et al., 2006). Gram-positive bacteria possess a thick cell wall of the peptidoglycan layer composed of linear polysaccharide chains, cross-linked by short peptides, which is a rigid structure that hinders the penetration of AgNPs into the bacterial cell wall, compared to Gram-negative bacteria where the cell wall consists of a thinner peptidoglycan layer (Rokade et al., 2016). Gram-positive bacteria have a thick cell wall of peptidoglycan composed of linear polysaccharide chains, with short peptides forming the cross-linkages, which is a firm structure that hinders the AgNPs from penetrating the bacterial cell wall, compared to Gram-negative bacteria where its cell wall consists of a thin layer of peptidoglycan (Loh et al., 2013).

3.5.3. Antifungal activity

The antifungal property of synthesized AgNPs was also studied. The synthesized AgNPs showed antifungal activity against pathogenic fungi, such as *F. oxysporum*, *A. alternata*, and *Trichoderma*, as shown in Table 1 and Fig. 8. Also, under experimental conditions, all tested fungi were inhibited to various extents using the particle of nanosilver and *C. myrrha* extract (Table 1; Fig. 8). The highest inhibition was found to be against *F. oxysporum* followed by *A. alternata* and *Trichoderma*.

3.6. Biochemical composition of C. myrrha extract

C. myrrha is classified under the genus *Commiphora* and family Burseraceae (Su et al., 2011). The composition of myrrh includes alcohol-soluble resins (25–40%), volatile oils (3–8%), and water-soluble gum (30–60%; Hanuš et al., 2005; Mekonnen, 2014; Tucker, 1986). The latter is composed of proteins and polysaccharides, whereas volatile oils include a mixture of terpenes, sterols, and steroids (Hanuš et al., 2005). The main component of myrrh aqueous extract is a polysaccharide with D-galactose, D-glucuronic acid, L-arabinose, and protein units (Fig. 9; Hough et al., 1952). The negative charge of AgNPs under alkaline pH [pH ¼ 8]. Thus, the biomolecules and phytochemicals may offer steric/electrostatic hindrance that acts as a repulsive spark against particle agglomeration. As a result, the capping and stabilization of nanoparticle are enhanced.

4. Conclusions

The anticancer activity of synthesized AgNPs against human cervical cancer cells could play an important role in the development of new therapeutic agents against cancer. Green synthesized AgNPs using myrrh aqueous extract have more promising antimicrobial activities against several pathogenic microbes. Myrrh aqueous extract can be used as a green reducing and covering agent for eco-friendly AgNP synthesis. The synthesized AgNPs showed good

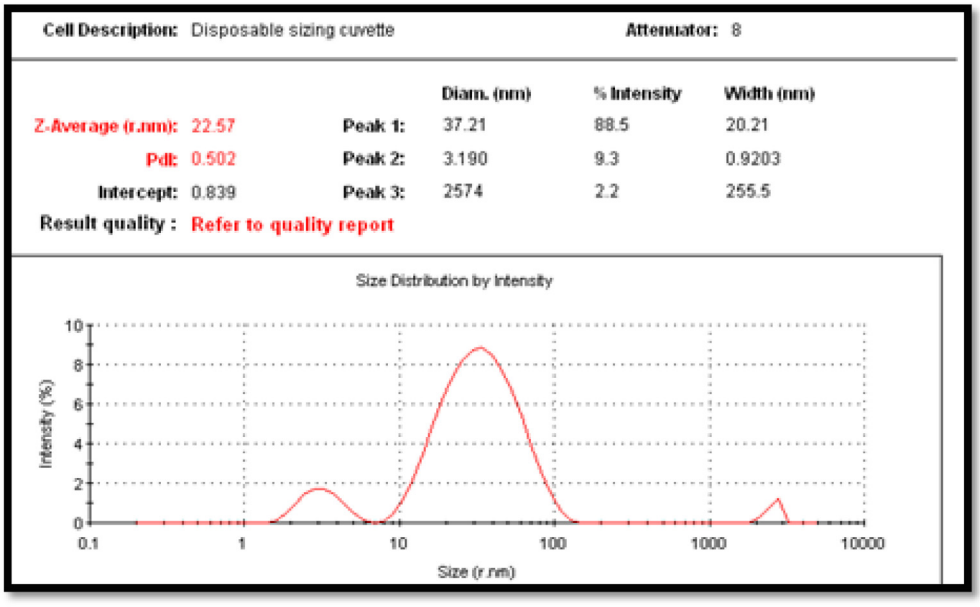

Fig. 4. Zeta sizer measurement of the average size of green silver nanoparticles size.

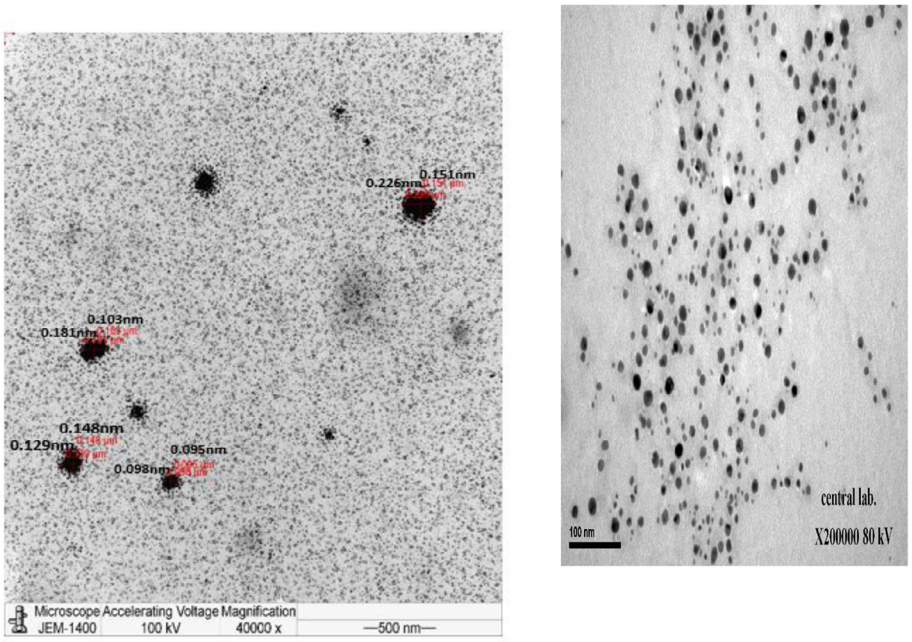

Fig. 5. Transmission Electron Microscopy images (TEM) images of silver nanoparticle.

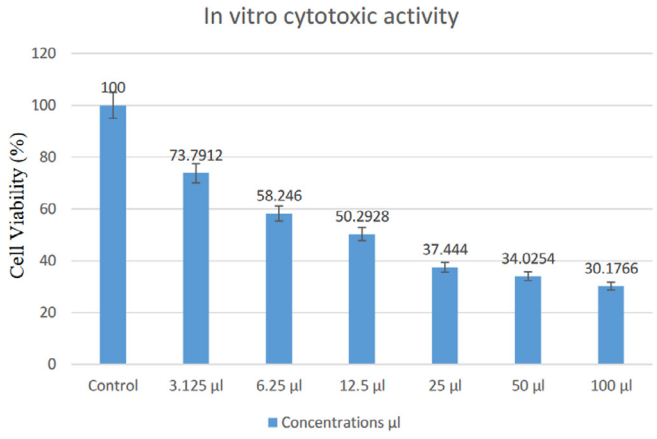

Fig. 6. In vitro cytotoxic activity of different concentration (3.125, 6.25, 12.5, 50, and 100 µl) from Ag NPs produced by myrrh extract against cells viability % for 48 h.

Table 1
Antifungal activity of the silver nanoparticles against different fungal organisms.

	Diameter of growth inhibition (mm)		
	A Pure extract of myrrh	B AgNPs of *C myrrh*	C control
Fusarium oxysporum	23	20	25
Alternaria alternata	16	14	18
Trichoderma	14	10	17

stability, and no visible changes were observed even after 4 months. AgNPs also have high bactericidal activity against both *E. faecalis* and *B. cereus* compared to myrrh aqueous extract, and antifungal activity improved with AgNPs. AgNPs can be tailor-made and used as antimicrobial agents for various biological and biomedical uses.

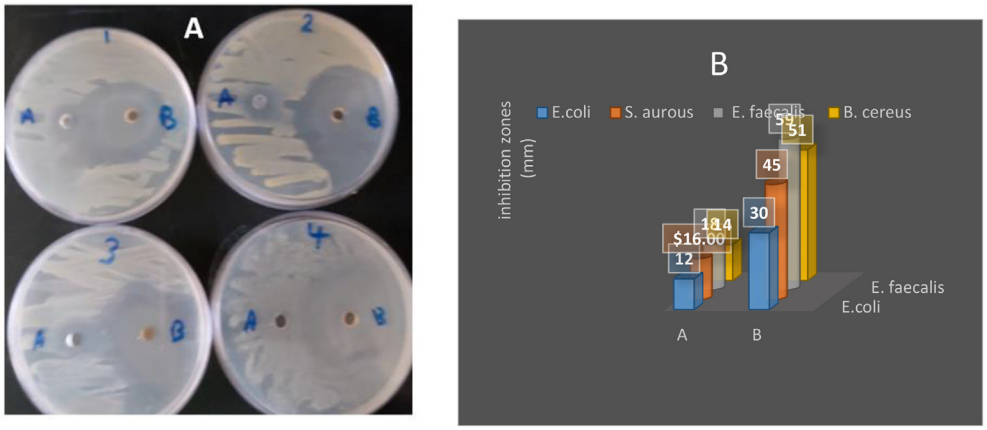

Fig. 7. Antibacterial activity of A) pure extract of myrrh and B) the synthesized AgNPs of myrrh and (1) *E. coli*, (2) *Staph. aurous*, (3) *E. faecalis* and (4) *B. cereus* (B) the values of inhibition zones (mm).

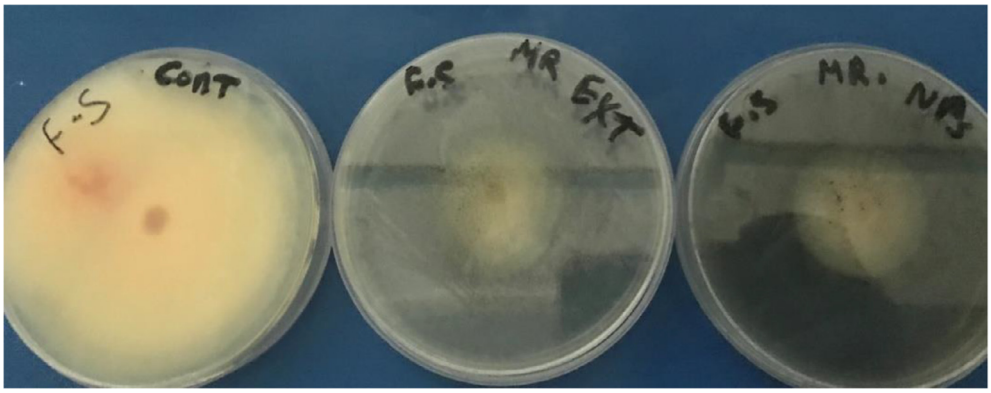

Fig. 8. Antifungal activity of the synthesized AgNPs of myrrh A), B) pure extract of myrrh *and* (C) control.

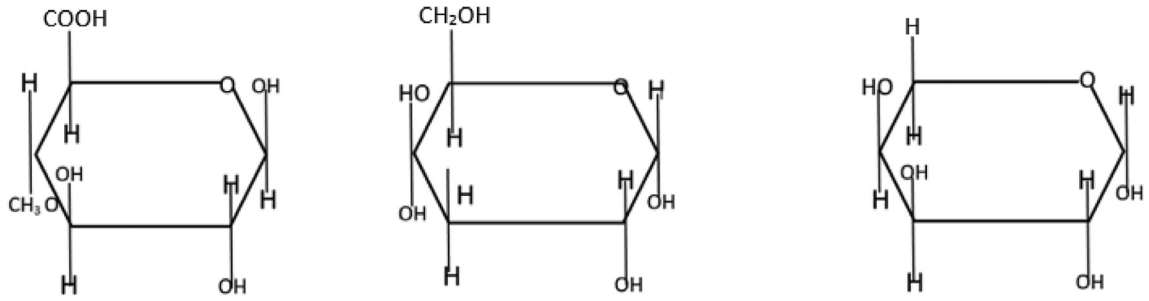

Fig. 9. Structures of saccharides in the myrrh extract (L to R: 4-methyl D-glucuronic acid, D-galactose, and L-arabinose) El-Sherbiny et al. (2013).

Declaration of Competing Interest

The authors declare that they have no known competing financial interests or personal relationships that could have appeared to influence the work reported in this paper.

Acknowledgements

Funding

This work was supported by the Deanship of Scientific Research at King Saud University for funding the work through research group project no. RG-1435-086.

Appendix A. Supplementary data

Supplementary data to this article can be found online at https://doi.org/10.1016/j.jksus.2020.09.024.

References

Ahmad, N., Bhatnagar, S., Ali, S.S., Dutta, R., 2015. Phytofabrication of bioinduced silver nanoparticle for biomedical applications. Int. J. Nanomed. 10, 7019.
Babich, H., Borenfreund, E., 1987. In vitro cytotoxicity of organic pollutants to bluegill sunfish (BF-2) cells. Environ. Res. 42, 229–237.
Bar, H., Bhui, D.K., Sahoo, G.P., Sarkar, P., De, S.P., Misra, A., 2009. Green synthesis of silver nanoparticle using latex of Jatropha curcas. Colloids Surf., A 339, 134–139.
Bawendi, M.G., Steigerwald, M.L., Brus, L.E., 1990. The quantum mechanics of larger semiconductor clusters ("Quantum Dots"). Annu. Rev. Phys. Chem. 41, 477–496.
Ben-Yehoshua, S., Borowitz, C., Hanuš, L.O., 2012. Frankincense, Myrrh, and Balm of Gilead: Ancient Spices of Southern Arabia and Judea, Horticultural Reviews, 1–76. John Wiley & Sons Inc.
Biswal, A.K., Misra, P.K., 2020. Biosynthesis and characterization of silver nanoparticle for prospective application in food packaging and biomedical applications. Mater. Chem. Phys. 123014.
De Heer, W.A., 1993. The physics of simple metal clusters: experimental aspects and simple models. Rev. Mod. Phys. 65, 611–676.
El-Sherbiny, I.M., Salih, E., Reicha, F.M., 2013. Green synthesis of densely dispersed and stable silver nanoparticle using myrrh extract and evaluation of their antibacterial activity. J. Nanostruct. Chem. 3, 8.
El Ashry, E., Rashed, N., Salama, O., Saleh, A., 2003. Components, therapeutic value and uses of myrrh. Die Pharmazie 58, 163–168.
Feng, Q.L., Wu, J., Chen, G., Cui, F., Kim, T., Kim, J., 2000. A mechanistic study of the antibacterial effect of silver ions on Escherichia coli and Staphylococcus aureus. J. Biomed. Mater. Res. 52, 662–668.
Ford, R., Api, A., Letizia, C., 1992. Fragrance raw material monographs: Lyral. Food Chem. Toxicol. 30, 49–51.
Gould, I.R., Lenhard, J.R., Muenter, A.A., Godleski, S.A., Farid, S., 2000. Two-electron sensitization: a new concept for silver halide photography. J. Am. Chem. Soc. 122, 11934–11943.
Hanuš, L.O., Řezanka, T., Dembitsky, V.M., Moussaieff, A., 2005. Myrrh-commiphora chemistry. Biomed Papers 149, 3–28.
Hösel, M., Krebs, F.C., 2012. Large-scale roll-to-roll photonic sintering of flexo printed silver nanoparticle electrodes. J. Mater. Chem. 22, 15683.
Hough, L., Jones, J., Wadman, W., 1952. Some observations on the constitution of gum myrrh. J. Chem. Soc. (Resumed), 796–800.
Inácio, P.L., Barreto, B.J., Horowitz, F., Correia, R.R.B., Pereira, M.B., 2013. Silver migration at the surface of ion-exchange waveguides: a plasmonic template. Opt. Mater. Exp. 3, 390.
Jensen, T.R., Malinsky, M.D., Haynes, C.L., Van Duyne, R.P., 2000. Nanosphere lithography: tunable localized surface plasmon resonance spectra of silver nanoparticle. J. Phys. Chem. B 104, 10549–10556.
Judd, W., Campbell, C.S., Kellogg E., Stevens P. 2002. Botanique systématique-Une perspective phylogénétique: 467p. De Boeck Université, Paris & Bruxelles.
Kaviya, S., Santhanalakshmi, J., Viswanathan, B., Muthumary, J., Srinivasan, K., 2011. Biosynthesis of silver nanoparticle using citrus sinensis peel extract and its antibacterial activity. Spectrochim. Acta Part A Mol. Biomol. Spectrosc. 79, 594–598.
Klaine, S.J., Alvarez, P.J.J., Batley, G.E., Fernandes, T.F., Handy, R.D., Lyon, D.Y., Mahendra, S., et al., 2008. Nanomaterials in the environment: behavior, fate, bioavailability, and effects. Environ. Toxicol. Chem. 27, 1825.
Le Ouay, B., Stellacci, F., 2015. Antibacterial activity of silver nanoparticle: a surface science insight. Nano Today 10, 339–354.
Loh, C.Y., Tan, Y.Y., Rohani, R., Weber, J.-F.R.F., Bhore, S.J., 2013. Diversity of endophytic bacteria in Malaysian plants as revealed by 16S rRNA encoding gene sequence based method of bacterial identification. J. Young Pharm. 5, 95–97.

Lu, H., Liu, S., Wang, X., Qian, X., Yin, J., Zhu, Z., 2003. Silver nanocrystals by hyperbranched polyurethane-assisted photochemical reduction of Ag+. Mater. Chem. Phys. 81, 104–107.
Lukman, A.I., Gong, B., Marjo, C.E., Roessner, U., Harris, A.T., 2011. Facile synthesis, stabilization, and anti-bacterial performance of discrete Ag nanoparticle using Medicago sativa seed exudates. J. Colloid Interface Sci. 353, 433–444.
Mekonnen, T., 2014. Evaluation of binding capacity of gum fraction of local myrrh (Commiphora myrrha Syn. C. molmol) in granule and tablet formulations. Addis Ababa University.
Noginov, M.A., Zhu, G., Bahoura, M., Adegoke, J., Small, C., Ritzo, B.A., Drachev, V.P., Shalaev, V.M., 2006. The effect of gain and absorption on surface plasmons in metal nanoparticle. Appl. Phys. B 86, 455–460.
Ramteke, C., Chakrabarti, T., Sarangi, B.K., Pandey, R.-A. 2012. Synthesis of silver nanoparticle from the aqueous extract of leaves of Ocimum sanctum for enhanced antibacterial activity. J. Chem. 2013.
Reddy, V.R., Currao, A., Calzaferri, G., 2007. Gold and silver metal nanoparticle-modified AgCl photocatalyst for water oxidation to O2. J. Phys. Conf. Ser. 61, 960–965.
Rokade, A.A., Patil, M.P., Yoo, S.I., Lee, W.K., Park, S.S., 2016. Pure green chemical approach for synthesis of Ag2O nanoparticle. Green Chem. Lett. Rev. 9, 216–222.
Saifuddin, N., Wong, C.W., Yasumira, A.A.N., 2009. Rapid biosynthesis of silver nanoparticle using culture supernatant of bacteria with microwave irradiation. E-J. Chem. 6, 61–70.
Saxena, A., Tripathi, R.M., Zafar, F., Singh, P., 2012. Green synthesis of silver nanoparticle using aqueous solution of Ficus benghalensis leaf extract and characterization of their antibacterial activity. Mater. Lett. 67, 91–94.
Shipway, A.N., Lahav, M., Willner, I., 2000. Nanostructured gold colloid electrodes. Adv. Mater. 12, 993–998.
Su, S., Wang, T., Duan, J.-A., Zhou, W., Hua, Y.-Q., Tang, Y.-P., Yu, L., Qian, D.-W., 2011. Anti-inflammatory and analgesic activity of different extracts of Commiphora myrrha. J. Ethnopharmacol. 134, 251–258.
Tsuji, T., Kakita, T., Tsuji, M., 2003. Preparation of nano-size particle of silver with femtosecond laser ablation in water. Appl. Surf. Sci. 206, 314–320.
Tucker, A.O., 1986. Frankincense and myrrh. Econ. Bot. 40, 425–433.
Xia, Y., Rogers, J.A., Paul, K.E., Whitesides, G.M., 1999. Unconventional methods for fabricating and patterning nanostructures. Chem. Rev. 99, 1823–1848.